Molecular and Cellular Endocrinology 547 (2022) 111594

Contents lists available at ScienceDirect

Molecular and Cellular Endocrinology

journal homepage: www.elsevier.com/locate/mce

SDHB and SDHD silenced pheochromocytoma spheroids respond differently to tumour microenvironment and their aggressiveness is inhibited by impairing stroma metabolism

Serena Martinelli [a], Maria Riverso [a], Tommaso Mello [a], Francesca Amore [a], Matteo Parri [a], Irene Simeone [a], Massimo Mannelli [a], Mario Maggi [a], Elena Rapizzi [b,*]

[a] Department of Experimental and Clinical Biomedical Sciences, University of Florence, Italy
[b] Department of Experimental and Clinical Medicine, University of Florence, Italy

ARTICLE INFO

Keywords:
Succinate dehydrogenase
Tumour migration
Spheroids
Tumour microenvironment
Pheochromocytoma/paraganglioma

ABSTRACT

Germline mutations in more than 20 genes, including those encoding for the succinate dehydrogenase (SDH), predispose to rare tumours, such as pheochromocytoma/paraganglioma (PPGL). Despite encoding for the same enzymatic complex, *SDHC* and *SDHD* mutated PHEO/PGLs are generally benign, while up to 80% of *SDHB* mutated ones are malignant.

In this study, we evaluated the different effects of tumour microenvironment on tumour cell migration/invasion, by co-culturing SDHB or SDHD silenced tumour spheroids with primary cancer-associated fibroblasts (CAFs). We observed that SDHD silenced spheroids had an intermediate migration pattern, compared to the highest migration capability of SDHB and the lowest one of the wild type (Wt) spheroids. Interestingly, we noticed that co-culturing Wt, SDHB and SDHD silenced spheroids with CAFs in low glucose (1 g/l) medium, caused a decreased migration of all the spheroids, but only for SDHB silenced ones this reduction was significant. Moreover, the collective migration, observed in high glucose (4.5 g/l) and characteristic of the SDHB silenced cells, was completely lost in low glucose. Importantly, migration could not be recovered even adding glucose (3.5 g/l) to low glucose conditioned medium.

When we investigated cell metabolism, we found that low glucose concentration led to a reduction of oxygen consumption rate (OCR), basal and maximal oxidative metabolism, and ATP production only in CAFs, but not in tumour cells. These results suggest that CAFs metabolism impairment was responsible for the decreased invasion process of tumour cells, most likely preventing the release of the pro-migratory factors produced by CAFs.

In conclusion, the interplay between CAFs and tumour cells is distinctive depending on the gene involved, and highlights the possibility to inhibit CAF-induced migration by impairing CAFs metabolism, indicating new potential therapeutic scenarios for medical therapy.

1. Introduction

Pheochromocytoma/paraganglioma (PPGL) are rare neuroendocrine tumours, generally benign, arising from neural crest derived cells. It has been demonstrated that PPGL are among the tumours most frequently accompanied by germline mutations. Indeed, more than 20 genes are responsible for a hereditary background in up to 40% of these tumours (Astuti et al., 2001; Baysal et al., 2000; Buffet et al., 2018; Burnichon et al., 2010; Calsina et al., 2018; Castro-Vega et al., 2014; Comino-Méndez et al., 2011; Crona et al., 2013; Dwight et al., 2018; Fishbein et al., 2015; Gaal et al., 2010; Hao et al., 2009; Kudryavtseva et al., 2019; Ladroue et al., 2008; Latif et al., 1993; Luchetti et al., 2015; Müller et al., 2005; Mulligan et al., 1993; Qin et al., 2010; Remacha et al. 2018, 2019; Wallace et al., 1990; Welander et al., 2018; Zhuang et al., 2012). These genes include those encoding the subunits of succinate dehydrogenase (SDH), also called mitochondrial complex II. Mutations in the *SDH* genes are currently the most common mutations found in PPGL.

SDH is located in the inner mitochondrial membrane and formed by four subunits, SDHA, B, C and D. Because of its role, both in the Krebs cycle and in the electron transport chain, SDH impairment induces deep

* Corresponding author. Dept. Experimental and Clinical Medicine, University of Florence, Viale Pieraccini 6, 50139 Firenze, Italy.
E-mail address: elena.rapizzi@unifi.it (E. Rapizzi).

https://doi.org/10.1016/j.mce.2022.111594
Received 30 April 2021; Received in revised form 11 January 2022; Accepted 4 February 2022
Available online 9 February 2022

changes in cell metabolism and functions (Eijkelenkamp et al., 2020). It is noteworthy, that almost 80% of *SDHB* mutated patients, but not those mutated in one of the other SDH subunits, develop metastatic lesions (Andrews et al., 2018). Undoubtedly, at present, one of the major open questions with PPGL is why *SDHB* mutated tumours are so aggressive compared to the tumours mutated in another subunit of the same enzymatic complex.

Although several hypotheses have been proposed, the precise mechanisms by which the impaired SDH activity leads to tumorigenesis and *SDHB* mutations to malignancy remain unknown (Moog et al., 2020). Tumour tissue analysis has shown that in SDH-mutated patients, regardless which subunit is mutated, SDH enzymatic activity is always decreased (Douwes Dekker et al., 2003; Rapizzi et al., 2012). In addition, the inhibition of SDH enzymatic activity is responsible for an increase in the expression of hypoxia inducible factors (HIFs) (Selak et al., 2005), DNA hypermethylation (Letouzé et al., 2013) and activation of angiogenesis. Moreover, Richter and colleagues (Richter et al., 2014) demonstrated that succinate:fumarate ratios were higher in both *SDHB*-mutated and metastatic tumours than in those due to *SDHD/C* mutations, suggesting that different additional pathways might be involved in tumour formation.

This scenario is even more complicated by the demonstration that SDHB silenced pheochromocytoma cells change the microenvironment properties, acquiring, in turn, a more aggressive phenotype (D'Antongiovanni et al., 2017). Over the last years, it has become increasingly evident the pivotal role of tumour microenvironment (TME) in promoting cancer cell growth and their metastatic spread (for recent reviews see: Dey et al., 2021; Farc and Cristea 2021). Tumour microenvironment has thus become a potential target for the therapy of certain tumours (recent reviews: Ganesh and Massagué 2021; Wu and Dai 2021).

Moreover, increasing consideration is being given to metabolic reprogramming of stromal cells present in the tumour microenvironment (Fiaschi et al., 2012; Gupta et al., 2017). For example, cancer-associated fibroblasts (CAFs), a major component in tumour stroma, have been reported to have increased glycolysis and produce high-energy nutrients that facilitate biogenesis in malignant cells, a process referred to as the "reverse Warburg effect" (Martinez-Outschoorn et al., 2011).

In the present study, we investigated the role of TME on SDHB or SDHD silenced spheroid growth and migration/invasion, by co-culturing spheroids with CAFs, providing new evidence that CAF metabolic reprogramming affects tumour aggressiveness.

2. Materials and methods

2.1. Cell transfection and clone selection for MTT SDHB and SDHD silencing

The MTT (pheochromocytoma mouse tumour tissue derived) cell line, generated by Martiniova and colleagues (Martiniova et al., 2009), and kindly provided by Arthur Tischler, was grown in DMEM supplemented with 10% FCS, 5% HS, 2 mM l-glutamine, 100 U/ml penicillin, and 100 μg/ml streptomycin at 37 °C in a 5% CO_2 humidified atmosphere. To establish a stable SDHB or SDHD silenced line, MTT cells were transfected at 90% confluency using Lipofectamine 3000 reagent (Thermo Fisher Scientific) according to the manufacturer's instructions, with a specific SDHB or SDHD Sure Silencing shRNA vector or a non-targeting shRNA construct (Qiagen) as negative control (Wt). Cells were maintained under selection with Puromycin (4 μg/ml) for 3 weeks. After selection, clones were grown in media with a lower amount of Puromycin for maintenance (1 μg/ml).

2.2. Fibroblasts isolation

Fibroblasts were obtained from legs of new born C57/BL mice (ethics approval prot. n. 577/2017) by enzymatic digestion with collagenase I (Sigma). The digestion was plated for 1 h at 37 °C then adherent cells, mostly fibroblasts, were washed twice in PBS and let grow in high glucose DMEM +10% FCS, 2 mM l-glutamine, 100 U/ml penicillin, and 100 μg/ml streptomycin at 37 °C in a 5% CO_2 humidified atmosphere.

2.3. Cell homogenates and lysates preparation

Homogenates and lysates were prepared as previously described (Rapizzi et al., 2014) with minor modifications. Clone pellets were homogenized in a solution containing 120 mM KCl, 20 mM HEPES, 2 mM $MgCl_2$, 1 mM EGTA, and 5 mg/ml BSA. The homogenates were centrifuged at 800 *g* for 10 min at 4 °C, and the enzyme assays were performed on the supernatant. For western blot analysis, cell pellets were lysed in buffer containing 50 mM Tris-HCl pH = 7.5, 120 mM NaCl, 1 mM EGTA, 6 mM EDTA, 15 mM $Na_4P_2O_7$, 20 mM NaF, and 1% Triton X-100 protease inhibitor cocktail. Lysates were clarified by centrifugation at 10 000 *g* for 15 min at 4 °C. Supernatants were quantified for protein content (Coomassie Blue reagent, Bio-Rad). All passages were carried out on ice.

2.4. Western blot analysis

Cell lysates (20 μg of proteins) were separated by SDS/PAGE and transferred onto PVDF (Immobilon, Billerica, Millipore, MA, USA), as previously described (Rapizzi et al., 2014). Bound antibodies were detected using ECL reagents (Immobilon) and analysed with a Bio-Rad ChemiDoc Imaging System (Quantity One) for dedicated chemiluminescent image acquisition. Densitometry was undertaken using ImageJ software. The polyclonals, anti-SDHB and anti-SDHD, were from Sigma Aldrich (HPA002868 and HPA045727, respectively), the mouse monoclonal anti-SDHA antibody was from Abcam (ab14715), the mouse monoclonal anti-HIF1α was from Santa Cruz Biotechnology (sc-13515). The polyclonal anti-actin and all the secondary antibodies, such as the anti-mouse, anti-rabbit, and anti-goat IgG HRP conjugated, were from Santa Cruz Biotechnology (sc-1615, sc-2005, sc-2004, sc-2020, respectively).

2.5. SDH activity

Cell homogenates (50 μg) were incubated in a phosphate buffer containing sodium azide, 2,6 dichlorophenolindophenol (DCPIP), sodium succinate, and phenazine methosulfate. Complex II specific activity was evaluated by photometry using the Victor3 1420 Multilabel Counter (Packard Instruments, PerkinElmer, Waltham MA, USA) to measure the decrease in absorbance that resulted from the oxidation of DCPIP at 600 nm (Rapizzi et al., 2015).

2.6. Gas Chromatography–Mass spectrometry (GC–MS)

For SCAN mode, 5×10^5 MTT cells were collected and subjected to extraction using a mixture of $CHCl_3$: MeOH: H_2O (1:1:1), before quenching with ice-cold MeOH: H_2O (1:1) containing norvaline, used as internal standard. $CHCl_3$ was then added, the samples were vortexed at 4 °C for 30 min, centrifuged at 3000 *g* for 10 min, and the aqueous phase was collected and allowed to evaporate at room temperature. Dried polar metabolites were dissolved in 60 μL of 2% methoxyamine hydrochloride in pyridine (Thermo Fisher) and held at 30 °C for 2 h. After dissolution and reaction, 90 μL N-Trimethylsilyl-N-methyl trifluoroacetamide (MSTFA) + 1% trimethylchlorosilane TMCS were added, and samples were incubated at 37 °C for 60 min. Gas chromatographic runs were performed with helium as carrier gas at 0.6 mL/min. The split inlet temperature was set to 250 °C and the injection volume of 1 μL. A split ratio of 1:10 was used. The GC oven temperature ramp was from 60 to 325 °C at 10 °C/min. The data acquisition rate was 10 Hz. For the Quadrupole, an Electron Ionization (EI) source (70eV)

was used, and full-scan spectra (mass range from 50 to 600) were recorded in the positive ion mode. The ion source and transfer line temperatures were set, respectively, to 250 and 290 °C. For the determination of relative metabolite abundances, the integrated signal of all ions for each metabolite fragment was normalized by the signal from norvaline and cell number (Richter et al., 2018).

2.7. Spheroids generation

To generate cancer spheroids, 5×10^3 tumour cells were added into each well of a round, low adherence, bottomed 96-well plates. Plates were then centrifuged at 220 *g* at room temperature for 10 min to initiate cell-cell interaction, and incubated at 37 °C, 5% CO_2. This procedure generated spheroids with homogeneous size and geometry (diameter ≥350 μm). After 48 h, spheroids were easily handled using a regular pipette without dissociating. Inverted microscopic analyses were routinely performed before each experiment to verify spheroid diameter. Only those with a diameter ≥350 μm were used (D'Antongiovanni et al., 2017).

2.8. Conditioned medium

To obtain conditioned medium, 2D co-cultures of mixed fibroblasts and tumour cells, in a 2:1 ratio, were plated and allowed to adhere overnight. Then, the culture medium was replaced with fresh DMEM containing 10% FCS and 4.5 g/l glucose or 1 g/l glucose. After 72 h, the conditioned medium was collected, centrifuged for 5 min at 232 *g* and used for further experiments.

2.9. 3D migration assays

To determine the effects of mouse primary fibroblasts on spheroid cell migration, spheroids were co-cultured with mouse primary fibroblasts using culture inserts (Greiner Bio-one) as previously described (D'Antongiovanni et al., 2017). Briefly, fibroblasts were seeded in 12-well plates (2.5×10^4, 7.5×10^4, 1.5×10^5, 3.5×10^5 cells/well), and the next day, they were pre-activated with 1 ml of conditioned medium (see above) with 4.5 g/l or 1 g/l of glucose for 24 h. At the same time, 100 μL of Corning Matrigel Basement Membrane Matrix (BD Biosciences) 0.3% solution was added to the growth surface of culture inserts for multiwell plates (transparent membrane with 3 μm pores), and let it to be hydrated overnight at 37 °C. Then, spheroids were selected and individually laid on the matrigel in the transwell insert and placed in the multiwell plates with (co-culture conditions) or without (for control conditions) fibroblasts. To determine the effects of succinate in high and low glucose DMEM, 20 mM of succinate were added or not to the media.

In another set of experiments, instead to performed co-cultures with fibroblasts, we evaluated migration using 1 ml of conditioned media (4.5 g/l or 1 g/l glucose) (see above), and to the 1 g/l conditioned medium, 3.5 g/l of glucose or 20 mM of lactate were added.

Bright field images of the spheroids were acquired by an AxioCam MRc digital camera for an inverted microscope Axiovert25 (Zeiss) at time 0. After 5 days, to evaluate migration, the spheroids were fixed with cold methanol and coloured using crystal violet staining, and new images were acquired. Using ImageJ software, migration areas were calculated as the difference between areas at day 0 and day 5 obtained by drawing circles around the spheroids at those times (D'Antongiovanni et al., 2017).

2.10. Spheroid cell number evaluation

To evaluate the number of spheroid cells at day 5 of migration, spheroids were laid on inserts coated with Matrigel and co-cultured or not with primary fibroblasts, as described above. After 5 days, spheroids were incubated at 4 °C for 45 min with Cell Recovery Solution (Corning, #354253), then harvested, washed in PBS, and centrifuged. Pellets were enzymatically digested, and the cells were counted.

2.11. Intracellular ATP

Intracellular ATP levels were measured using CellTiter-Glo luminescent cell viability assay (Promega). This assay was performed according to the manufacturer's protocol. Briefly, tumour cells and fibroblasts were seeded separately into 96-well plates. After 16 h, cells were washed twice in PBS, and left to grow in DMEM with high (4.5 g/l) or low (1 g/l) glucose. Moreover, to evaluate the effects of pyruvate and lactate on fibroblast ATP production, 40 mM of pyruvate or 40 mM of lactate were added to the 1 g/l glucose conditioned medium. After 72 h, 3 wells/condition were washed twice in PBS, and 125 μl PBS +125 μl of CellTiter-Glo reagent were added to each well. The culture plates were shaken at 300 rpm for 5 min and then incubated at room temperature for 25 min to stabilize the luminescent signal. Luminescence was measured using the Victor3 1420 Multilabel Counter (Packard Instruments, PerkinElmer), and other 3 wells/condition were counted and used for normalization.

2.12. Seahorse XFe96 metabolic assay

For the XF Mito Stress test, cells or spheroids were cultured in a high (4.5 g/l) or low (1 g/l) glucose medium for 72 h. Medium was then replaced with XF base medium supplemented with 2 mM glutamine, 1 mM sodium pyruvate and with 4.5 g/l glucose or with 1 g/l glucose. Cells or spheroids were incubated for 1 h at 37 °C in a non-CO_2 incubator before the analysis. Mito Stress test reveals basal respiration, maximal respiration and the ability of the cells to exploit mitochondrial oxidative metabolism. These analyses were performed by real-time measurement oxygen consumption rate (OCR) after a sequential injection of compounds that interfere with the electron transport chain: oligomycin (0.5 μM), carbonyl cyanide-4 (trifluoromethoxy) phenylhydrazone (FCCP) (1 μM) and Rotenone/Antimycin A (0.5 μM). Protein quantification was used to normalize the results of Mito Stress test.

2.13. Immunofluorescence staining

The 0.3% matrigel solution was added to the growth surface of chambers slides (Nunclon Sphera, Thermo Fisher) and let to be hydrated for 1 h at 37 °C, then single spheroids were laid on the Matrigel, let them stand for 3 h, and next 4.5 g/l glucose or 1 g/l glucose conditioned medium (see above) was added. After 5 days, spheroids were fixed with 4% paraformaldehyde for 10 min, followed by permeabilization in PBS with 0.1% Triton X-100 for 45 min at room temperature. Spheroids were then incubated for 1 h at 37 °C with phalloidin fluorescein isothiocyanate labeled (Sigma-Aldrich) to visualize actin filaments, and with TO-PRO-3 iodide (Life Technologies) for nuclei staining. Confocal images were acquired with a Leica SP2-AOBS, as follows. HC PL fluotar 20 × 0.5 NA objective, voxel size x = 0.732 μm, y = 0.732 μm, z = 0.814 μm; HCX PL APO 63 × 1.4 NA objective, voxel size x = 0.232 μm, y = 0.232 μm, z = 0.244 μm. Images were prepared for publication using the Fiji software (Schindelin et al., 2012) and are shown as maximum intensity projection along the *z*-axis.

2.14. Mitotracker fluorescence analysis

Primary fibroblasts (3×10^4) were cultured on 35 mm u-Dish (Ibidi GmbH) in a high (4.5 g/l) or low (1 g/l) glucose medium for 72 h, and then stained for 30 min with 200 nM Mitotracker Deep Red FM (Invitrogen, Thermofisher). Thereafter, medium was replaced with fresh pre-warmed DMEM, without phenol red, supplemented with 10% FCS, and cells were immediately imaged using an inverted Leica DMI6000 microscope equipped with a stage incubator (Pecon) with controlled temperature, humidity and CO_2. Images were captured through a 63 × 1.2 NA water immersion objective, with a DFC350FX camera and Leica

filter set Y5. All image analysis was performed using ImageJ software.

2.15. Statistical analysis

Data analyses were performed by the computer program GraphPad Prism Version 8.3.0 for Windows (GraphPad Software). The statistical significance of value differences was evaluated by one-way ANOVA followed by Bonferroni's or Tukey's multiple comparison test or by *t*-test. A *P* value of less than 0.05 was considered significant.

3. Results

3.1. Characterization of SDHB and SDHD silenced cells

In SDHB or SDHD silenced cells, the SDHB or SDHD protein expression levels were reduced of about 80% and 64%, respectively (Fig. 1A–B). Moreover, we observed that the silencing did not affect the expression of the other subunits (SDHD and SDHA in SDHB silenced cells, and SDHB and SDHA in SDHD silenced ones). We then investigated in cell homogenates the functional implication of the silencing. Functional impairment was confirmed by a significant reduction of SDH enzymatic activity, 46% for SDHB and 42% for SDHD silenced cells compared with their Wt counterpart (Fig. 1C–D). Although in the two cell populations, the silencing caused a similar deficiency in the SDH activity, only the SDHB silenced cells showed a significant increase in the succinate:fumarate ratio compared with Wt ($p < 0.05$) (Fig. 1 E). Nevertheless, HIF1α protein expression level was found increased, despite not significantly from Wt, in both SDHB and SDHD silenced cells (Fig. 1F–G).

3.2. SDHB and SDHD silenced spheroids show different aggressiveness in the presence of fibroblasts

To evaluate the aggressive potential of SDHB and SDHD silenced spheroids, we studied migration/invasion of extracellular matrix, here represented by matrigel, of single cultured spheroids and of spheroids co-cultured with CAFs. Wt, SDHB or SDHD silenced single cultured spheroids did not show significant differences in migration (Fig. 2 A), as also demonstrated by the computation of the migratory areas (Fig. 2 B). On the contrary, when spheroids were co-cultured with CAFs, we did not only detect a clear and significant detachment of tumour cells invading the surrounding space in all the spheroids (Fig. 2A–B), but we also observed that this matrix invasion was significantly different depending on the tumour cell types. In particular, SDHD silenced spheroids showed an intermediate trend in the migratory pattern compared with Wt and SDHB silenced spheroids. Indeed, the migration areas of SDHD silenced cells were significantly higher compared with Wt, but significantly lower compared with SDHB silenced spheroids (Fig. 2 B). Moreover, we found that spheroid migration areas directly correlated with the number of fibroblasts present in the co-cultures (Fig. 2 C). Indeed, increasing the fibroblast amount from $2{,}5 \times 10^4$ to $1{,}50 \times 10^5$ caused almost a linear rise of SDHB silenced spheroid migration areas. This increase was

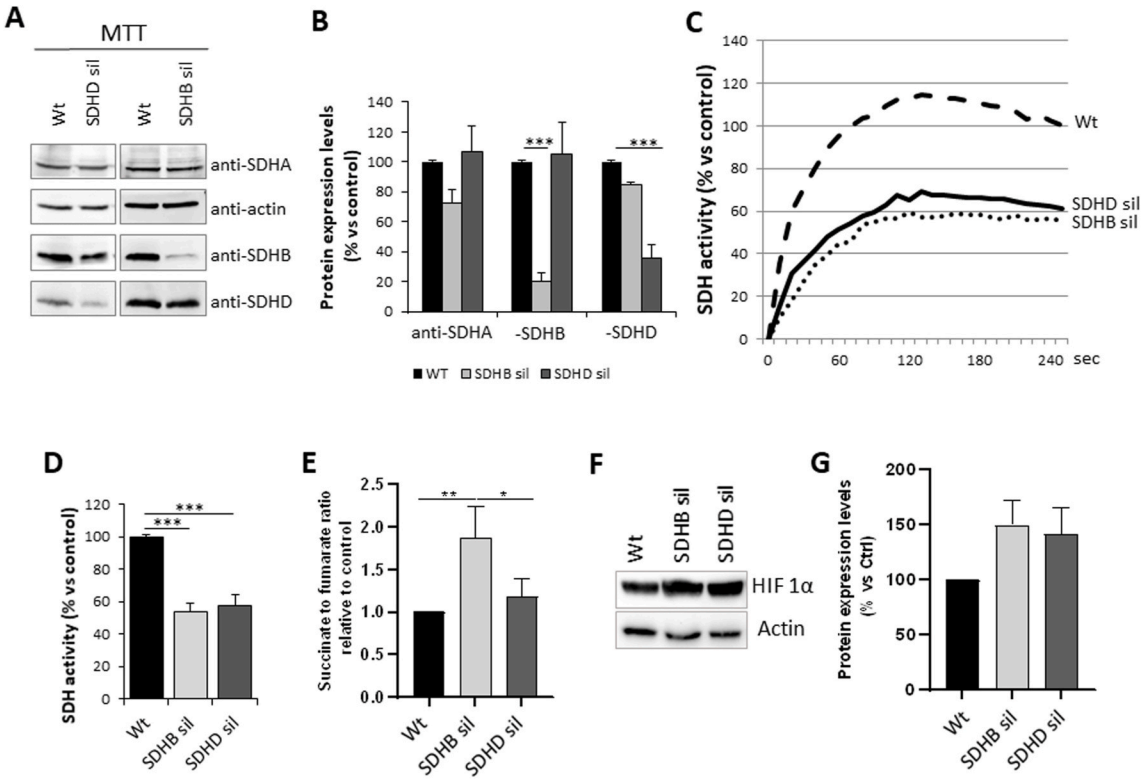

Fig. 1. Characterization of stable SDHB and SDHD silenced cell lines. (A) Representative blots of the expression of mitochondrial SDHA, B and D subunits. (B) Densitometric analysis of western blot bands, performed by Bio-Rad imaging and analysis software (Quantity One), showed significant differences in the SDHB and SDHD subunit expression levels in SDHB (light grey) and in SDHD silenced cells (dark grey) respectively, compared to Wt (black). Bars are the means of three independent preparations ± SD, ***$p < 0.001$. (C) Representative traces of SDH enzymatic activity measured in cell homogenates. The silenced SDHB and SDHD cells (dotted and continuous lines, respectively) showed a similar decrease of the SDH activity, significantly different compared with Wt (dashed line). (D) Histogram represents the SDH activity expressed as the percentages. SDHB and SDHD silenced cells (light and dark grey, respectively) showed a significantly decreased of SDH activity compared to Wt (black). Bars are the means of three independent experiments (each of them conducted in duplicate samples) ± SD, ***$p < 0.01$. (E) The bar graph represents the means of intracellular succinate/fumarate ratio ± SD, measured by GC/MS, in three independent experiments with two replicates. SDHB silenced cells (light grey) showed a significant increase of the metabolites ratio compared with both Wt (black) and to SDHD silenced cells (dark grey), *$p < 0.05$, **$p < 0.01$. (F) Representative immunoblot of HIF1α expression in Wt, SDHB and SDHD silenced cells. (G) Optical density analysis of western blot bands. Actin immunoblots was used as loading control. For all the analyses One-way ANOVA post-test Bonferroni was used.

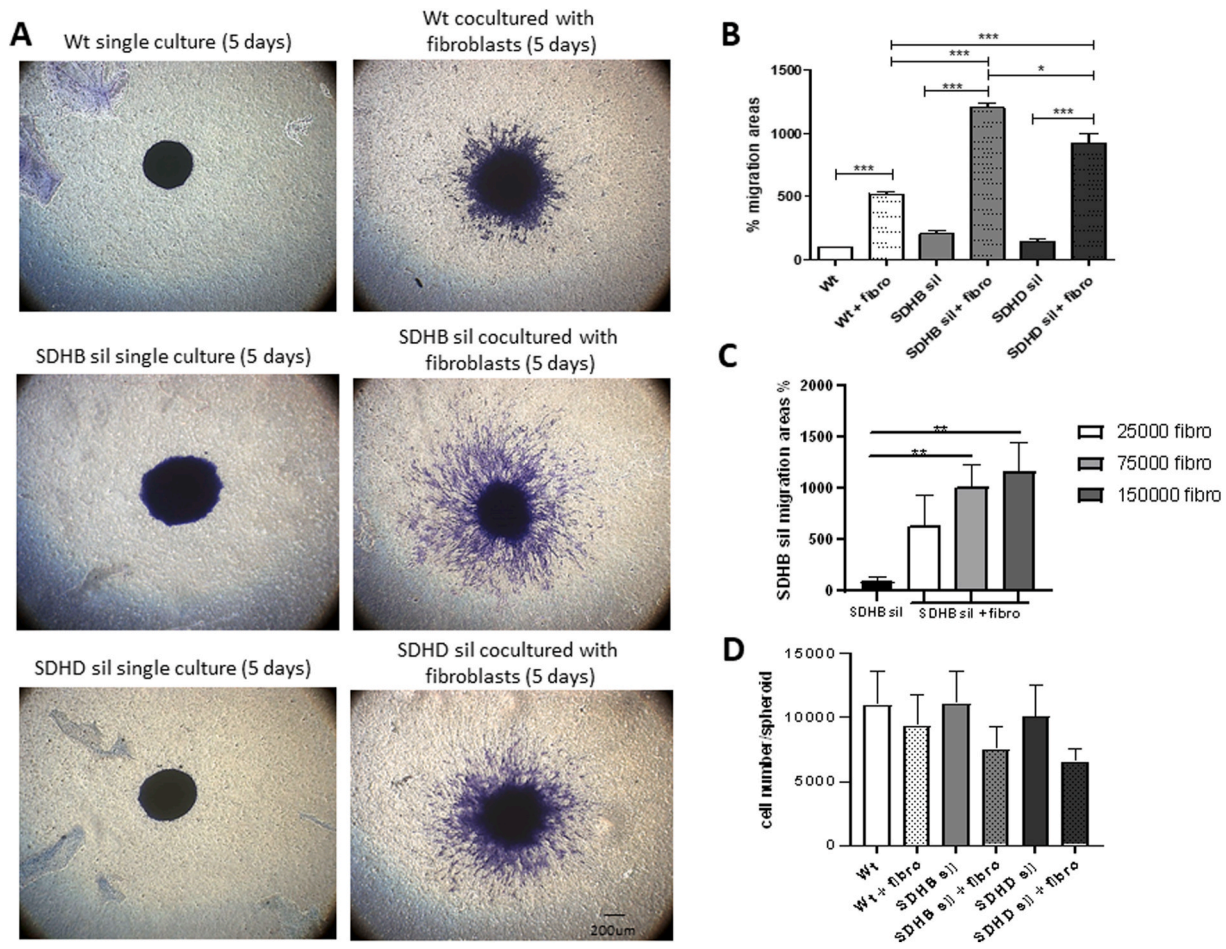

Fig. 2. Effects of the microenvironment on tumour spheroid migration. (A) 5x images of spheroids laid on 0.3% matrigel in the upper compartment of transwell insert. The migration capability was observed after 5 days. In single culture, spheroids migrating cells were barely detectable. If spheroids were cultured in presence of activated fibroblasts (CAFs) plated in the lower compartment, an evident detachment of clusters of cells in the surrounding space was observed. The computation of the spheroids migratory areas (B) was calculated as the difference between areas at day 0 and day 5. The migration process was always significantly increased if spheroids were co-cultured with CAFs. Nevertheless, the effect of the microenvironment was significantly more evident in SDHB silenced spheroids (dotted light grey bars) compared with Wt (dotted white grey bars) and SDHD silenced (dotted dark grey bars) spheroids. Bars are the means of three independent experiments, each performed in duplicates ± SEM, *$p < 0.05$, ***$p < 0.001$ (One-way ANOVA post-test Bonferroni). (C) Computational analysis of the migration areas after 5 days of SDHB silenced spheroids co-cultured with $2,5 \times 10^4$ (white bar), $7,5 \times 10^4$ (white grey bar) or with $1,5 \times 10^5$ (grey bar) CAFs. The migration process showed an increasing size of the areas depending by CAFs concentration, and become statistically significant, compared with control, starting from co-cultures with $7,5 \times 10^4$ CAFs. Bars are the means of three independent experiments, each performed in duplicates ±SEM, **$p < 0.01$ (One-way ANOVA post-test Tukey). (D) Wt, SDHB and SDHD silenced spheroid cell count after 5 days of single culture or co-cultured with CAFs. Bars are the means of three independent experiments, each performed in duplicates ± SEM (One-way ANOVA post-test Tukey).

statistically significant, compared with single cultured spheroid areas, starting from co-cultures with $7,5 \times 10^4$ fibroblasts (Fig. 2 C). Furthermore, to understand if cell spreading was due to migration and/or proliferation, we counted the spheroid cells after 5 days of single cultures or co-cultures with CAFs. We observed that the number of cells was comparable among the Wt, SDHB and SDHD silenced spheroids in single cultures, similarly to what detected in the co-cultures. Interestingly, co-cultured spheroids showed a smaller number of cells compared to their single cultured counterpart, suggesting that proliferation and migration are mutually exclusive (Fig. 2 D).

3.3. Lowering glucose concentration negatively affects spheroid migration and changes SDHB collective migration

Since SDHB silenced cells showed an intracellular increase of the oncometabolite succinate compared to both SDHD silenced and Wt spheroids, we hypothesized that this metabolite could be partially responsible for the significant increased migration of SDHB silenced cells. In humans, circulating levels of succinate range from 2 to 20 μM and can increase up to 8.7 mM under certain circumstances (Grimolizzi and Arranz 2018; Matlac et al., 2021). For this reason, we performed the migration assay adding 20 mM of succinate to the co-culture media of Wt, SDHB, SDHD silenced spheroids and CAFs. Nevertheless, in this experimental condition, we did not appreciate any difference in migration among the different co-cultures (Fig. 3 A). We then supposed that the high glucose (4.5 g/l) concentration plus 10% serum in the medium and the presence of CAFs, could already induce a maximal migration, possibly masking any succinate effects. Thus, we performed the experiments substituting a high glucose medium with a low glucose (1 g/l) medium. Even in this case, we did not observe an increase in migration due to succinate administration, but, unexpectedly, we noticed that in low glucose all the spheroids (Wt, SDHB and SDHD silenced ones) showed a reduction of the migratory areas compared to those measured in high glucose (Fig. 3 A). SDHB silenced spheroids showed the greatest reduction in spread area (3.5 fold compared to high-glucose medium), whereas in the SDHD silenced and in the Wt spheroids was of about 2.1 and 2.8, respectively. Besides, in low glucose, migration dissimilarities were no longer appreciable; in fact, the

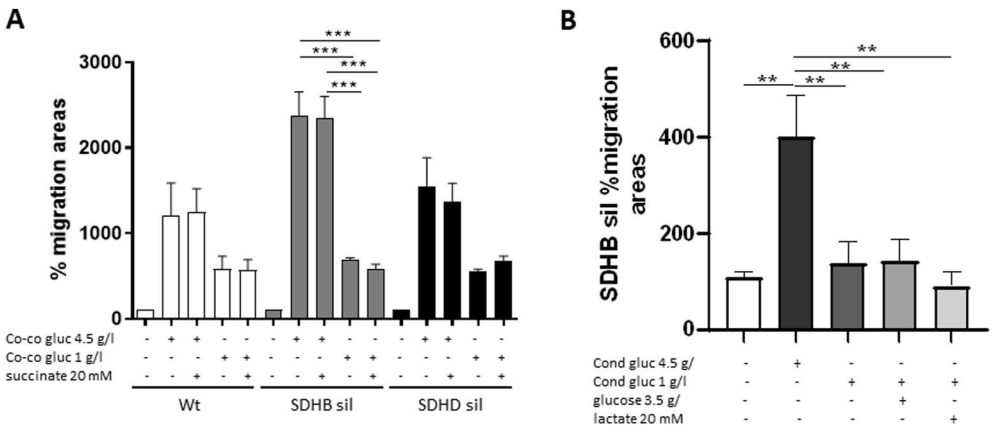

Fig. 3. Effects of glucose and succinate on tumour spheroid migration. Computational analysis of the migration areas after 5 days of different culturing conditions. (A) In this first set of experiments, spheroids were single cultured or co-cultured with CAFs. All the spheroids, Wt (white), SDHB (light grey), and SDHD (dark grey) silenced spheroids, showed a decreased migration process in low glucose (1 g/l) compared to that in high glucose (4.5 g/l). This reduction was significant in SDHB silenced spheroids. The migration process was not affected, by adding succinic acid to both 4.5 g/l and 1 g/l glucose culture media, in all the spheroids. Bars are the means of three independent experiments, each performed in duplicates ± SEM, ***p < 0.0001 (One-way ANOVA post-test Tukey). (B) In this second set of experiments, spheroids were cultured without (white bar) or with high (4.5 g/l, black bar) or low (1 g/l, grey bar) glucose CAFs conditioned media. Moreover, low glucose CAFs conditioned media was supplemented or not with 3.5 g/l glucose (light grey bar) or 20 mM lactate (white grey bar). SDHB migration was not recovered following the supplement of either 3.5 g/l glucose or 20 mM lactate. Bars are the means of three independent experiments, each performed in duplicates ± SEM, **p < 0.005 (One-way ANOVA post-test Tukey).

migration areas were comparable among all the different cell types.

To assess if the reduced migration in low glucose medium was caused by the reduced nutritional condition, we supplemented the low (1 g/l) glucose medium with either glucose (3.5 g/l) or lactate (20 mM), and performed 3D migration assay on SDHB silenced spheroid. Interestingly, in both cases the simple addition of these substrates was not sufficient to recover migration (Fig. 3 B).

We have recently demonstrated, that Wt and SDHB silenced CAFs conditioned spheroids developed long filamentous formations, along which tumour cells migrated from the spheroid into the Matrigel. Most importantly, while Wt cells moved along them in a single cell manner, SDHB silenced cells showed a collective migration (D'Antongiovanni et al., 2017). Remarkably, when we compared migration performed in low glucose (1 g/l) conditioned medium, we observed that SDHB

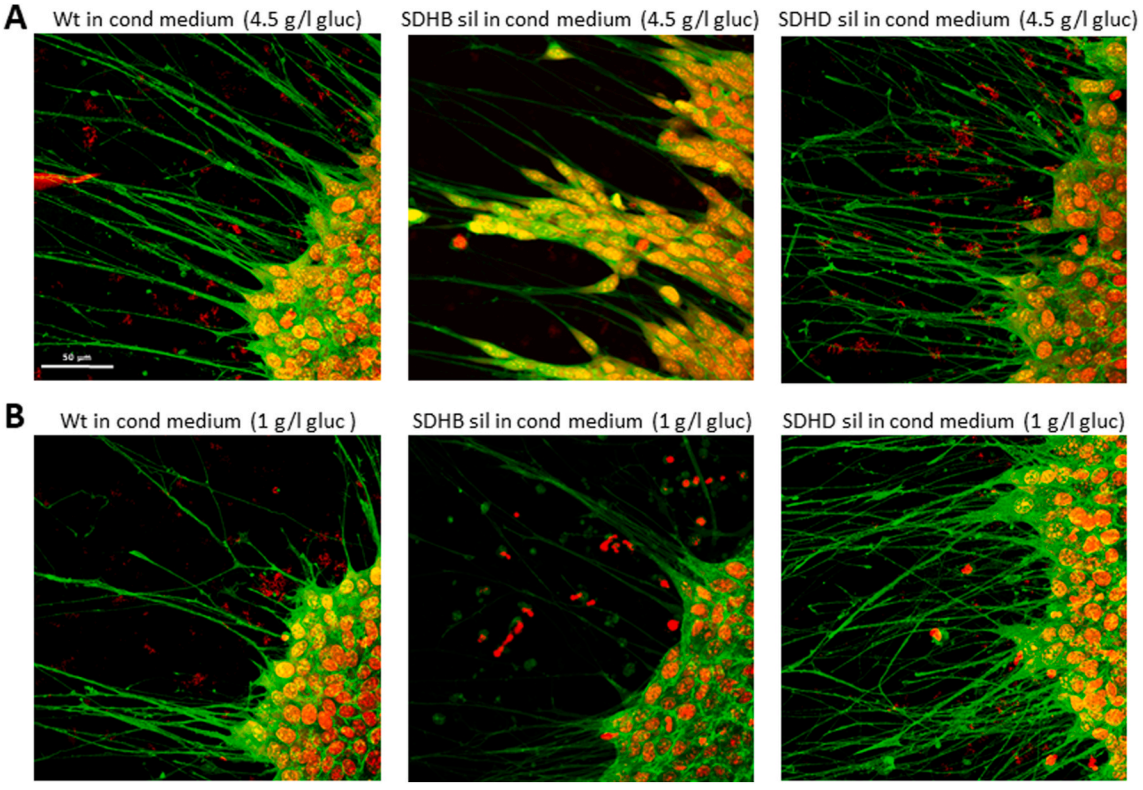

Fig. 4. Characterization of tumour spheroid migration by confocal microscopy. Spheroids were labeled with phalloidin fluorescein isothiocyanate to visualize actin filaments (in green), and with TO-PRO™-3 iodide for nuclei staining (in red). Confocal images were acquired with a Leica SP2-AOBS, processed using Fiji software, and shown as maximum intensity projection along the z-axis. (A) When spheroids were grown in high (4.5 g/l) glucose SDHB silenced spheroids, but no Wt and SDHD silenced ones, migrate in a collective way. (B) The collective migration was affected by low glucose (1 g/l) conditioned medium. After 5 days of migration in low glucose conditions, SDHB silenced spheroids lost their capability to migrate in clusters. Images are representative of three independent experiments. (For interpretation of the references to colour in this figure legend, the reader is referred to the Web version of this article.)

silenced spheroids completely lost their ability to migrate collectively, despite their outgrowth formations were not significantly different from those found in high glucose (4.5 g/l) (Fig. 4). Moreover, herein, we observed that also SDHD silenced cells developed long outgrowth processes, but interestingly, cells moved along them individually, resembling the Wt spheroids behaviour (Fig. 4).

3.4. Low glucose changes fibroblast metabolism

We first measured the intracellular ATP concentration in fibroblasts, Wt, SDHB and SDHD silenced cells grown in high (4.5 g/l) and low (1 g/l) glucose media. Interestingly, we observed that ATP concentration was similar among Wt, SDHB and SDHD silenced cells, whatever was the glucose concentration in the medium (Fig. 5 A). On the contrary, fibroblasts showed a significant reduction of ATP concentration when cultured in low glucose, compared with that in high glucose counterpart (Fig. 5 A). We looked in depth into fibroblasts metabolism changes, by using the Seahorse Analyzer. Oxygen consumption rate (OCR) was measured in real-time, throughout the sequential administration of oligomycin, FCCP and Rotenone/Antimycin A. Fibroblasts, cultured in low glucose, showed an overall reduced OCR, a lower respiratory activity at baseline, reduced maximal respiratory capacity and ATP production compared with those in high glucose (Fig. 5B–C).

We also investigated the OCR profile in Wt, SDHB and SDHD silenced spheroid or cell monolayer grown in high (4.5 g/l) or low (1 g/l) glucose medium (Supplementary Data, Figs. 1 and 2, respectively). In all the tumour samples, the oxidative phosphorylation profile was similar in both culturing conditions. In fact, we did not observe any significative changes in the ATP production, baseline respiratory rate l and maximal respiration capacity, thus confirming that only fibroblast metabolism deeply depends on glucose availability.

3.5. Low glucose does not impair fibroblast mitochondria

We investigated if the decreased glucose concentration might possibly induce fibroblasts mitochondrial damage. To address this hypothesis, we cultured fibroblasts in high (4.5 g/l) or low (1 g/l) glucose and examined mitochondrial morphology by MitoTracker labelling (Fig. 6 A). We observed that, in both culturing conditions, the mitochondrial architecture was characterized by the classic rod-shaped structure, demonstrating that mitochondria organization was maintained even in low glucose medium. Next, we evaluated if mitochondria were able to restore their intracellular ATP concentration when the low glucose medium was supplemented with two alternative carbon sources, such as pyruvate or lactate (Fig. 6 B). Intriguingly, while the supplement of lactate did not boost ATP concentration, the addition of pyruvate induced a significative increase of intracellular ATP, which however, still remained significantly lower than the ATP concentration measured in cells grown in 4.5 g/l glucose.

4. Discussion

In this study, we show, for the first time, that SDHD silenced tumour cells respond differently to TME stimuli compared with SDHB silenced ones. We demonstrate that the extraordinary increase of spheroid cell migration/invasion induced by TME, here represented by primary CAFs, is significantly reduced in SDHD silenced spheroids compared with SDHB silenced ones. Furthermore, we observe that the outgrowth processes, most likely used as tracks for cell migration, are considerably induced by TME in all the cases, but only SDHB silenced cells migrate

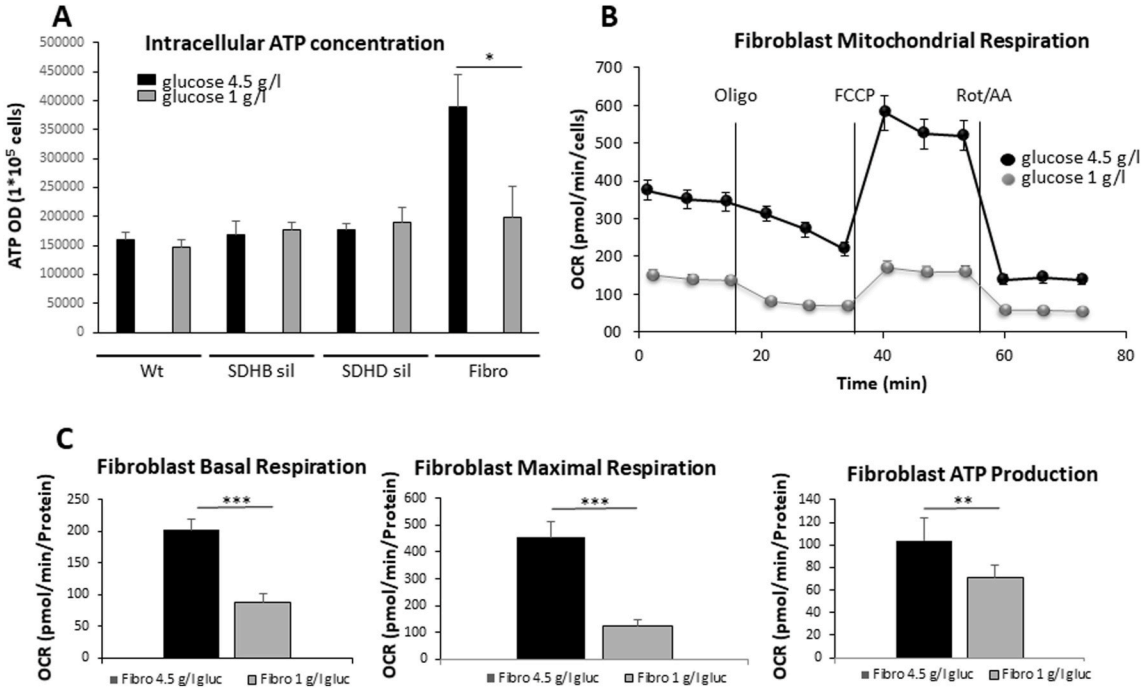

Fig. 5. Effects of low (1 g/l) glucose on intracellular ATP concentration and its impact on fibroblasts metabolism. (A) Intracellular ATP concentration. Culturing tumour cells in low glucose (1 g/l, grey bars) medium did not affect the intracellular ATP content. On the contrary, culturing primary fibroblasts in low glucose induced a significant intracellular ATP concentration reduction compared with ATP in cells cultured in high glucose (4.5 g/l, black bars). ATP level was measured using Cell titer Glow (Promega) and normalized on cell number. Bars are the means of three independent experiments (each of them conducted in duplicate) ± SD, *p < 0.05) (Two tailed paired *t*-test). (B and C) Low glucose status affects glucose dependent oxidative phosphorylation in fibroblasts. Cells were subjected to Seahorse XFe96 Mito Stress Test analysis and oxygen consumption rate (OCR) was measured in real time and normalized on protein levels. Basal, maximal respiration and ATP production was calculated as described in Material and Methods, based on the OCR after the administration of the adenosine triphosphate ATP synthase inhibitor oligomycin, the proton uncoupler carbonilcyanide p-triflouromethoxyphenylhydrazone (FCCP), and the respiratory complex I inhibitor rotenone, together with the respiratory complex III inhibitor antimycin A. Each dot represents six technical replicates from three biological replicates. Data represent means ± SD, **p < 0.01, ***p < 0.001 (Two tailed *t*-test).

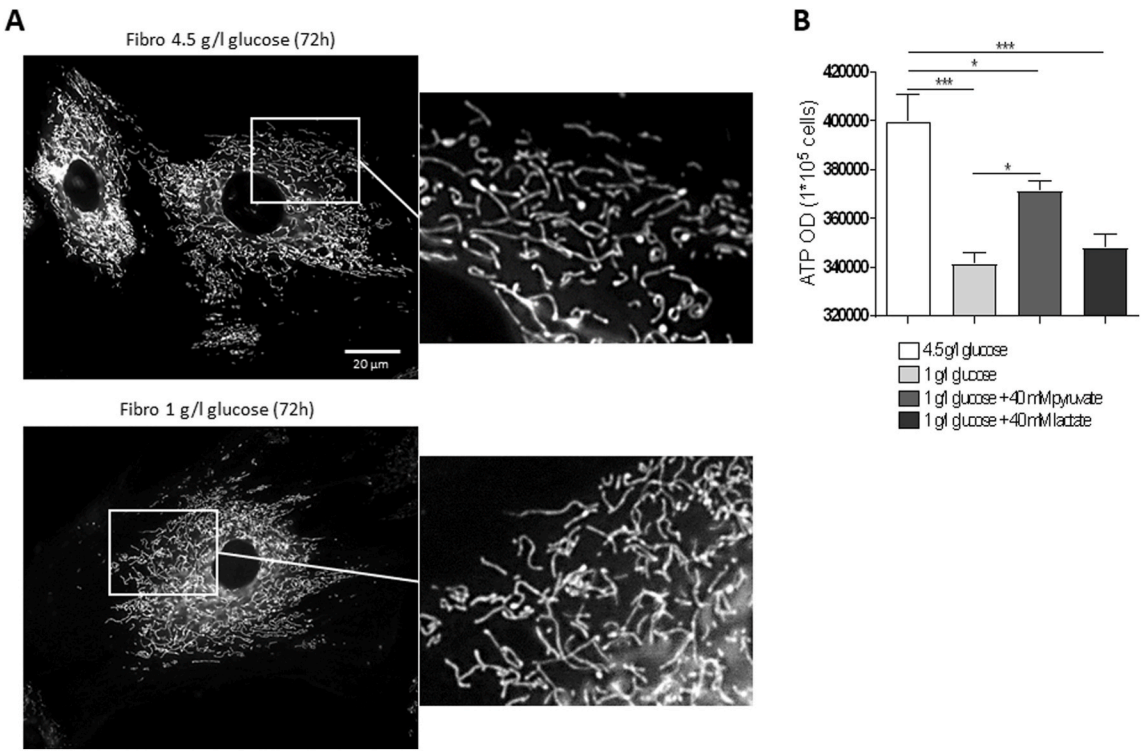

Fig. 6. Fibroblast mitochondria function and morphology. (A) Effect of high (4.5 g/l) or low (1 g/l) glucose on mitochondrial homeostasis. Mitochondria were visualized by MitoTracker Deep Red labelling. Organelle structure and intracellular distribution were maintained even in low glucose condition. (B) Fibroblast intracellular ATP concentration decreased significantly in cells cultured in low (white grey bar) glucose compared with that in cells in high (white bar) glucose. The addition of 40 mM pyruvate (grey bar) to low glucose medium induced a significant increase of intracellular ATP concentration compared with that measured in low glucose medium. But still, ATP was significantly lower compared with that detected in high glucose. The addition of 40 mM lactate (black bar) to low glucose medium did not affect ATP production. ATP levels were measured using Cell titer Glow (Promega) and normalized on cell number. Bars are the means of three independent experiments (each of them conducted in duplicate) ± SEM, *$p < 0.05$, ***$p < 0.0001$ (One-way ANOVA post-test Tukey).

collectively. In addition, we report that low glucose concentration alters CAFs metabolism, which, in turn, impairs the capability of fibroblasts to produce and release pro-migratory factors.

It is well known that PPGL aggressiveness depends on which susceptibility gene is mutated. It is particularly interesting that tumours mutated for genes encoding for the different subunits of the same enzyme, such as the SDH, show a completely different ability to spread and metastasize. Indeed, tumours mutated for SDHC or SDHD are usually benign, whereas those mutated for SDHB are very often malignant (Timmers et al., 2007). The molecular mechanisms responsible for such a difference are mostly unknown, as well as the metabolic and functional differences between benign and malignant SDHx mutated tumours. From tumour tissue analysis, we have previously shown that in SDHx mutated patients, regardless which subunit is mutated, SDH enzymatic activity is always decreased (Rapizzi et al., 2012). Moreover, we have also demonstrated that SDH deficient PPGL are characterized by 25 fold higher succinate tissue levels than tumours without SDHx mutations, and importantly, that the succinate:fumarate ratios are higher in SDHB mutated tumours than in those carrying SDHC/D mutations (Richter et al., 2014). The accumulation of succinate within the tumour cells modulates a wide spectrum of pathways ranging from the pseudo-hypoxia response to epigenetic reprogramming (Eijkelenkamp et al., 2020). Letouzé and colleagues (Letouzé et al., 2013) showed that the DNA and histone hypermethylation is significantly higher in SDHB mutated tumours compared with other SDHx mutated ones. The authors suggest that SDH inactivation may be more complete in SDHB mutated tumours, leading to a higher succinate accumulation and hence to a stronger inhibition of the demethylation. In line with this hypothesis, we show that succinate:fumarate intracellular ratio is significantly increased in SDHB silenced cells, compared to both Wt and SDHD silenced cells. However, investigating the functional effect of SDH silencing on pseudo hypoxia, we observed that HIF-1α protein expression is similarly increased in both SDHB and SDHD silenced cells compared with Wt. This result suggests that, the partial reduction of SDH activity observed in our cell lines, is anyway sufficient to induce a biological response in both SDHB and SDHD silenced cells. Nevertheless, the simple supplementation of the oncometabolite succinate to the medium is not enough to increase either SDHD silenced or Wt cell migration. This observation is very interesting, since indicates that at least *in vitro*, measuring only the overall steady state succinate:fumarate levels and HIF-1α expression is inadequate for predicting the cellular phenotype.

Solid tumours are very complex tissues, which include not only cancer cells, but also non-malignant stromal cells such as macrophages, endothelial cells, fibroblasts, immune cells, and extracellular matrix, forming the so-called TME (Hanahan and Coussens 2012). CAFs are the most abundant cell population within the TME in most cancers (Chen and Song 2019), playing a pivotal role in tumour cell migration and invasion (Erez et al., 2010; Olumi et al., 1999). We previously demonstrated (D'Antongiovanni et al., 2017) that primary CAFs, plays a specific role in increasing the migration properties of spheroid and that this effect is extraordinarily enhanced in SDHB silenced ones. Moreover, we found that only SDHB silenced spheroids migrate in a collective manner, showing that SDHB silenced cells migrate as clusters of cells. In this study, we highlighted the driving effect of the TME in promoting spheroid migration, by the demonstration that SDHB silenced spheroids migration area is directly proportional to the number of CAFs in the co-culture. Intriguingly, we show that TME induces migration also of SDHD silenced spheroids, but although this phenomenon is significantly higher to that observed in Wt, is still significantly lower to that of SDHB

silenced ones. Noteworthy, it is also different the modality of cell migration. Indeed, only SDHB silenced cells, but not SDHD silenced ones, show a collective invasion of the matrix. Collective cell migration is a fundamental process, that represents a coordinated movement of groups of cells connected to each other by cell-cell junctions (Hegerfeldt et al., 2002; Wolf et al., 2007; Zhu et al., 2015). It has been reported that this type of migration is related to cancer migration and metastatic potential (Zhang et al., 2019). Furthermore, it has been described, that cells presenting a collective migration have higher invasive capacity and higher resistance to the clinical treatments than those showing a single cell tumour migration (Yang et al., 2019). Since *SDHB* mutated PPGL are more aggressive than those mutated in other susceptibility genes, our data on the exclusive SDHB related collective migration, confirm and support what has been stated in the literature.

In PPGL, it has never been observed the development of neurite-like structures nor clusters of cells collectively migrating along them that might recall the type of migration herein described. In 1972, Angeletti and colleagues (Angeletti et al., 1972) reported that normal adrenal chromaffin cells and their neoplastic counterparts in pheochromocytoma did not possess neural processes *in vivo*. Moreover, *in vivo*, normal adrenal chromaffin cells did not form neural outgrowths following to nerve growth factor (NGF) treatment (Angeletti et al., 1972). Interestingly, few years later, Greene and Tischler (1976) demonstrated that, *in vitro*, almost the 80% of rat pheochromocytoma PC12 cells, exposed to NGF for 7 days, developed neural-like processes. Therefore, it is reasonable hypothesise that pheochromocytoma cells consequently to CAFs released factors are able to form neural-like outgrowths used by cells to migrate only *in vitro*. *In vivo*, tumour chromaffin cells might not produce neurite-like structures, nevertheless, in presence of TME tumour cells might change their characteristics acquiring specific migration mechanisms.

In this work, we also demonstrate that the observed migration event is really due to moving cells, and is not a false result related to proliferating cells. Certainly, the total number of cells of the migrating spheroids is even slightly lower compare with the total amount of not migrating spheroid cells. This data is in accordance with the literature, since it is well known., that proliferation and migration are mutually exclusive: the high motility suppresses cell proliferation and *vice versa* (Fedotov and Iomin, 2008). This phenomenon is known as the migration-proliferation dichotomy. The permissiveness of the TME may promote migration while decreasing proliferation (Giese et al., 2003). Therefore, tumour cell invasion is probably stimulated by soluble factors produced by CAFs in response to cancer-derived cytokines, acting in a paracrine, autocrine or juxtacrine fashion (Cangkrama et al., 2020; Kojima et al., 2010; Li et al., 2019). Indeed, CAFs may induce metabolic and functional changes of tumour cells by producing and releasing a plethora of growth factors, chemokines, cytokines and metabolites (Najafi et al., 2019).

While normal cells rely mainly on Krebs cycle and OXPHOS as an efficient source of ATP, tumour cells are required to reprogram their metabolism to meet the enhanced energy requirement of cell division, the increased biosynthesis of macromolecules, for anabolic processes and the tight regulation of redox status, which they primarily do through the 'Warburg Effect" (Warburg et al., 1927). Metabolic fuels, produced by the glycolytic active CAFs, are taken up by the neighbouring tumour cells in a process called the 'Reverse Warburg Effect' to increase their tumorigenic and metastatic potential (Lisanti et al., 2013). We observed that migration of all tumour spheroids is reduced in low glucose, and this effect is particularly evident in SDHB silenced spheroids. Moreover, SDHB silenced cells completely lose their capability to move in a collective manner, when kept in low glucose.

We speculated that the inhibition of cell migration observed in low glucose medium could be caused by a reduction of intracellular ATP in cancer cells. This was not the case, because interestingly, we observe a significant decrease in intracellular ATP levels only in fibroblasts, but not in tumour cells, cultured in low glucose. These results are in line with the observation that if glucose-independent metabolism is characteristic of tumour cells, this is not true for fibroblasts. CAFs are not transformed cells and rely mainly on Krebs cycle and OXPHOS. Thus, they are particularly sensitive to glucose concentration in the medium. These data strongly suggest that affecting CAF metabolism, by decreasing the glucose medium concentration, CAFs are no longer able to produce and secrete critical molecules for cell migration. Consequently, the invasion ability of tumour spheroids to invade the matrix is significantly impaired. This assumption is confirmed by the impossibility to re-establish migration areas, restoring high glucose concentration by addition of 3.5 g/l glucose to 1 g/l conditioned medium.

Interestingly, under low glucose conditions, fibroblast mitochondria decrease their ATP synthesis, but maintained their integrity, as demonstrated by the study of mitochondrial morphology and intracellular distribution. In addition, fibroblast mitochondria are able to partially recover ATP production if low glucose medium is supplemented with pyruvate, suggesting that also the mitochondrial activity is preserved. Supplementing low glucose medium with lactate, the intracellular ATP concentration is not affected, and further experiments are needed to understand that this might be explained by the fact that CAFs might use lactate for other purposes.

Taken together, this data demonstrates that SDHD and SDHB silenced cells show a different functional response to the pro-migration drivers produced by CAFs, highlighting the relevance of the TME contribution to the aggressiveness of SDHB silenced cells, and confirming that tumour stroma cells are a promising therapeutic target for cancer treatment.

Funding

This work was supported by the Paradifference Foundation, and by AIRC under IG 2020 - ID. 24820 project. S.M., M.M. and E.R. are members of the ENS@T (European Network for the Study of Adrenal Tumours). S.M., M.M., M.M. and E.R. are members of the Florence Center of Excellence recognized by the European Network for the Study of Adrenal Tumours (ENS@T).

CRediT authorship contribution statement

Serena Martinelli: conceived and designed the experiments, Formal analysis, performed the experiments, acquired and analysed the data, Writing – original draft, drafted: revised the manuscript. **Maria Riverso:** Formal analysis, performed the experiments, acquired and analysed the data. **Tommaso Mello:** Formal analysis, performed the experiments, acquired and analysed the data. **Francesca Amore:** Formal analysis, performed the experiments, acquired and analysed the data. **Matteo Parri:** Formal analysis, performed the experiments, acquired and analysed the data. **Irene Simeone:** performed the experiments, acquired and analysed the data. **Massimo Mannelli:** helped with constructive discussions. **Mario Maggi:** helped with constructive discussions. **Elena Rapizzi:** conceived and designed the experiments, revised the manuscript.

Aknowledgements

We wish to thank Dr. Arthur Tischler, who kindly provided the pheochromocytoma mouse tumour tissue derived (MTT) cells, generated by Martiniova and colleagues (Martiniova et al., 2009).

Appendix A. Supplementary data

Supplementary data to this article can be found online at https://doi.org/10.1016/j.mce.2022.111594.

References

Andrews, K.A., Ascher, D.B., Pires, D.E.V., Barnes, D.R., Vialard, L., Casey, R.T., Bradshaw, N., Adlard, J., Aylwin, S., Brennan, P., Brewer, C., Cole, T., Cook, J.A., Davidson, R., Donaldson, A., Fryer, A., Greenhalgh, L., Hodgson, S.V., Irving, R., Lalloo, F., McConachie, M., McConnell, V.P.M., Morrison, P.J., Murday, V., Park, S. M., Simpson, H.L., Snape, K., Stewart, S., Tomkins, S.E., Wallis, Y., Izatt, L., Goudie, D., Lindsay, R.S., Perry, C.G., Woodward, E.R., Antoniou, A.C., Maher, E.R., 2018. Tumour risks and genotype–phenotype correlations associated with germline variants in succinate dehydrogenase subunit genes SDHB, SDHC and SDHD. J. Med. Genet. 55, 384–394. https://doi.org/10.1136/jmedgenet-2017-105127.

Angeletti, P.U., Levi-Montalcini, R., Kettler, R., Thoenen, H., 1972. Comparative studies on the effect of the nerve growth factor on sympathetic ganglia and adrenal medulla in newborn rats. Brain Res. 44, 197–206. https://doi.org/10.1016/0006-8993(72)90375-7.

Astuti, D., Latif, F., Dallol, A., Dahia, P.L., Douglas, F., George, E., Sköldberg, F., Husebye, E.S., Eng, C., Maher, E.R., 2001. Gene mutations in the succinate dehydrogenase subunit SDHB cause susceptibility to familial pheochromocytoma and to familial paraganglioma. Am. J. Hum. Genet. 69, 49–54. https://doi.org/10.1086/321282.

Baysal, B.E., Ferrell, R.E., Willett-Brozick, J.E., Lawrence, E.C., Myssiorek, D., Bosch, A., van der Mey, A., Taschner, P.E., Rubinstein, W.S., Myers, E.N., 2000. Mutations in SDHD, a mitochondrial complex II gene, in hereditary paraganglioma. Science 287, 848–851. https://doi.org/10.1126/science.287.5454.848.

Buffet, A., Morin, A., Castro-Vega, L.J., Habarou, F., Lussey- Lepoutre, C., Letouzé, E., Lefebvre, H., Guilhem, I., Haissaguerre, M., Raingeard, I., 2018. Germline mutations in the mitochondrial 2-Oxoglutarate/malate carrier *SLC25A11* gene confer a predisposition to metastatic paragangliomas. Cancer Res. 78, 1914–1922. https://doi.org/10.1158/0008-5472.can-17-2463.

Burnichon, N., Brière, J.J., Libé, R., Vescovo, L., Rivière, J., Tissier, F., Jouanno, E., Jeunemaitre, X., Bénit, P., Tzagoloff, A., Rustin, P., Bertherat, J., Favier, J., Gimenez-Roqueplo, A.P., 2010. SDHA is a tumor suppressor gene causing paraganglioma. Hum. Mol. Genet. 19, 3011–3020. https://doi.org/10.1093/hmg/ddq206.

Calsina, B., Currás-Freixes, M., Buffet, A., Pons, T., Contreras, L., Letón, R., Comino-Méndez, I., Remacha, L., Calatayud, M., Obispo, B., 2018. Role of MDH2 pathogenic variant in pheochromocytoma and paraganglioma patients. Genet. Med. 20, 1652–1662. https://doi.org/10.1038/s41436-018-0068-7.

Cangkrama, M, Wietecha, M., Mathis, N., Okumura, R., Ferrarese, L., Al-Nuaimi, D., Antsiferova, M., Dummer, R., Innocenti, M., Werner, S., 2020. A paracrine activin A-mDia2 axis promotes squamous carcinogenesis via fibroblast reprogramming. EMBO Mol. Med. 12, e11466 https://doi.org/10.15252/emmm.201911466.

Castro-Vega, L.J., Buffet, A., De Cubas, A.A., Cascón, A., Menara, M., Khalifa, E., Amar, L., Azriel, S., Bourdeau, I., Chabre, O., Currás-Freixes, M., Franco-Vidal, V., Guillaud-Bataille, M., Simian, C., Morin, A., Letón, R., Gómez-Graña, A., Pollard, P. J., Rustin, P., Robledo, M., Favier, J., Gimenez-Roqueplo, A.P., 2014. Germline mutations in FH confer predisposition to malignant pheochromocytomas and paragangliomas. Hum. Mol. Genet. 23, 2440–2446. https://doi.org/10.1093/hmg/ddt639.

Chen, X., Song, E., 2019. Turning foes to friends: targeting cancer-associated fibroblasts. Nat. Rev. Drug Discov. 18, 99–115. https://doi.org/10.1038/s41573-018-0004-1.

Comino-Méndez, I., Gracia-Aznárez, F.J., Schiavi, F., Landa, I., Leandro-García, L.J., Letón, R., Honrado, E., Ramos-Medina, R., Caronia, D., Pita, G., Gómez-Graña, A., de Cubas, A.A., Inglada-Pérez, L., Maliszewska, A., Taschin, E., Bobisse, S., Pica, G., Loli, P., Hernández-Lavado, R., Díaz, J.A., Gómez-Morales, M., González-Neira, A., Roncador, G., Rodríguez-Antona, C., Benítez, J., Mannelli, M., Opocher, G., Robledo, M., Cascón, A., 2011. Exome sequencing identifies MAX mutations as a cause of hereditary pheochromocytoma. Nat. Genet. 663–667. https://doi.org/10.1038/ng.861, 1943.

Crona, J., Delgado Verdugo, A., Maharjan, R., Stålberg, P., Granberg, D., Hellman, P., Björklund, P., 2013. Somatic mutations in H-RAS in sporadic pheochromocytoma and paraganglioma identified by exome sequencing. J. Clin. Endocrinol. Metab. 98, E1266–E1271. https://doi.org/10.1210/jc.2012-4257.

Dey, P., Kimmelman, A.C., DePinho, R.A., 2021. Metabolic codependencies in the tumor microenvironment. Cancer Discov. 11, 1–15. https://doi.org/10.1158/2159-8290.CD-20-1211.

Douwes Dekker, P.B., Hogendoorn, P.C., Kuipers-Dijkshoorn, N., Prins, F.A., van Duinen, S.G., Taschner, P.E., Van der Mey, A.G.L., Cornelisse, C.J., 2003. SDHD mutations in head and neck paragangliomas result in destabilization of complex II in the mitochondrial respiratory chain with loss of enzymatic activity and abnormal mitochondrial morphology. J. Pathol. 201, 480–486. https://doi.org/10.1002/path.1461.

Dwight, T., Flynn, A., Amarasinghe, K., Benn, D.E., Lupat, R., Li, J., Cameron, D.L., Hogg, A., Balachander, S., Candiloro, I.L.M., 2018. TERT structural rearrangements in metastatic pheochromocytomas. Endocr. Relat. Cancer 25, 1–9. https://doi.org/10.1530/erc-17-0306.

D'Antongiovanni, V., Martinelli, S., Richter, S., Canu, L., Guasti, D., Mello, T., Romagnoli, P., Pacak, K., Eisenhofer, G., Mannelli, M., Rapizzi, E., 2017. The microenvironment induces collective migration in SDHB-silenced mouse pheochromocytoma spheroids. Endocr. Relat. Cancer 24, 555–564. https://doi.org/10.1530/ERC-17-0212.

Eijkelenkamp, K., Osinga, T.E., Links, T.P., van der Horst-Schrivers, A.N.A., 2020. Clinical implications of the oncometabolite succinate in SDHx-mutation carriers. Clin. Genet. 97, 39–53. https://doi.org/10.1111/cge.13553.

Erez, N., Truitt, M., Olson, P., Arron, S.T., Hanahan, D., 2010. Cancer-associated fibroblasts are activated in incipient neoplasia to orchestrate tumor-promoting inflammation in an NF-kappaB-dependent manner. Cancer Cell 17, 135–147. https://doi.org/10.1016/j.ccr.2009.12.041.

Farc, O., Cristea, V., 2021. An overview of the tumor microenvironment, from cells to complex networks. Exp. Ther. Med. 21, 96. https://doi.org/10.3892/etm.2020.9528.

Fedotov, S., Iomin, A., 2008. Probabilistic approach to a proliferation and migration dichotomy in the tumor cell invasion. Phys. Rev. E - Stat. Nonlinear Soft Matter Phys. 77, 031911 https://doi.org/10.1103/PhysRevE.77.031911.

Fiaschi, T., Marini, A., Giannoni, E., Taddei, M.L., Gandellini, P., De Donatis, A., Lanciotti, M., Serni, S., Cirri, P., Chiarugi, P., 2012. Reciprocal metabolic reprogramming through lactate shuttle coordinately influences tumor-stroma interplay. Cancer Res. 72, 5130–5140. https://doi.org/10.1158/0008-5472.CAN-12-1949.

Fishbein, L., Khare, S., Wubbenhorst, B., DeSloover, D., D'Andrea, K., Merrill, S., Cho, N. W., Greenberg, R.A., Else, T., Montone, K., LiVolsi, V., Fraker, D., Daber, R., Cohen, D.L., Nathanson, K.L., 2015. Whole-exome sequencing identifies somatic ATRX mutations in pheochromocytomas and paragangliomas. Nat. Commun. 6, 6140. https://doi.org/10.1038/ncomms7140.

Gaal, J., Burnichon, N., Korpershoek, E., Roncelin, I., Bertherat, J., Plouin, P.F., de Krijger, R.R., Gimenez-Roqueplo, A.P., Dinjens, W.N., 2010. Isocitrate dehydrogenase mutations are rare in pheochromocytomas and paragangliomas. J. Clin. Endocrinol. Metab. 95, 1274–1278. https://doi.org/10.1210/jc.2009-2170.

Ganesh, K., Massagué, J., 2021. Targeting metastatic cancer. Nat. Med. 27, 34–44. https://doi.org/10.1038/s41591-020-01195-4.

Giese, A., Bjerkvig, R., Berens, M.E., Westphal, M., 2003. Cost of migration: invasion of malignant gliomas and implications for treatment. J. Clin. Oncol. 21, 1624–1636. https://doi.org/10.1200/JCO.2003.05.063.

Greene, L.A., Tischler, A.S., 1976. Establishment of a noradrenergic clonal line of rat adrenal pheochromocytoma cells which respond to nerve growth factor. Proc. Natl. Acad. Sci. U.S.A. 73, 2424–2428. https://doi.org/10.1073/pnas.73.7.2424.

Grimolizzi, F., Arranz, L., 2018. Multiple faces of succinate beyond metabolism in blood. Haematologica 103, 1586–1592. https://doi.org/10.3324/haematol.2018.196097.

Gupta, S., Roy, A., Dwarakanath, B.S., 2017. Metabolic cooperation and competition in the tumor microenvironment: implications for therapy. Front. Oncol. 7, 68. https://doi.org/10.3389/fonc.2017.00068.

Hanahan, D., Coussens, L.M., 2012. Accessories to the crime: functions of cells recruited to the tumor microenvironment. Cancer Cell 21, 309–322. https://doi.org/10.1016/j.ccr.2012.02.022.

Hao, H.X., Khalimonchuk, O., Schraders, M., Dephoure, N., Bayley, J.P., Kunst, H., Devilee, P., Cremers, C.W., Schiffman, J.D., Bentz, B.G., Gygi, S.P., Winge, D.R., Kremer, H., Rutter, J., 2009. SDH5, a gene required for flavination of succinate dehydrogenase, is mutated in paraganglioma. Science 325, 1139–1142. https://doi.org/10.1126/science.1175689.

Hegerfeldt, Y., Tusch, M., Bröcker, E.-B., Friedl, P., 2002. Collective cell movement in primary melanoma explants plasticity of cell-cell interaction, β1-integrin function, and migration strategies. Cancer Res. 62, 2125–2130.

Kojima, Y., Acar, A., Eaton, E.N., Mellody, K.T., Scheel, C., Ben-Porath, I., Onder, T.T., Wang, Z.C., Richardson, A.L., Weinberg, R.A., Orimo, A., 2010. Autocrine TGF-β and stromal cell-derived factor-1 (SDF-1) signaling drives the evolution of tumor-promoting mammary stromal myofibroblast. Proc. Natl. Acad. Sci. U.S.A. 107, 20009–20014. https://doi.org/10.1073/pnas.1013805107.

Kudryavtseva, A.V., Lukyanova, E.N., Kalinin, D.V., Zaretsky, A.R., Pokrovsky, A.V., Golovyuk, A.L., Fedorova, M.S., Pudova, E.A., Kharitonov, S.L., Pavlov, V.S., Kobelyatskaya, A.A., Melnikova, N.V., Dmitriev, A.A., Polyakov, A.P., Alekseev, B.Y., Kiseleva, M.V., Kaprin, A.D., Krasnov, G.S., Snezhkina, A.V., 2019. Mutational load in carotid body tumor. BMC Med. Genom. 2, 39. https://doi.org/10.1186/s12920-019-0483-x.

Ladroue, C., Carcenac, R., Leporrier, M., Gad, S., Le Hello, C., Galateau-Salle, F., Feunteun, J., Pouysségur, J., Richard, S., Gardie, B., 2008. PHD2 mutation and congenital erythrocytosis with paraganglioma. N. Engl. J. Med. 359, 2685–2692. https://doi.org/10.1056/NEJMoa0806277.

Latif, F., Tory, K., Gnarra, J., Yao, M., Duh, F.M., Orcutt, M.L., Stackhouse, T., Kuzmin, I., Modi, W., Geil, L., 1993. Identification of the von Hippel-Lindau disease tumor suppressor gene. Science 260, 1317–1320. https://doi.org/10.1126/science.8493574.

Letouzé, E., Martinelli, C., Loriot, C., Burnichon, N., Abermil, N., Ottolenghi, C., Janin, M., Menara, M., Nguyen, A.T., Benit, P., Buffet, A., Marcaillou, C., Bertherat, J., Amar, L., Rustin, P., De Reyniès, A., Gimenez-Roqueplo, A.P., Favier, J., 2013. SDH mutations establish a hypermethylator phenotype in paraganglioma. Cancer Cell 23, 739–752. https://doi.org/10.1016/j.ccr.2013.04.018.

Li, Z., Zhang, J., Zhou, J., Lu, L., Wang, H., Zhang, G., Wan, G., Cai, S., Du, J., 2019. Nodal facilitates differentiation of fibroblasts to cancer-associated fibroblasts that support tumor growth in melanoma and colorectal cancer. Cells 8, 538. https://doi.org/10.3390/cells8060538.

Lisanti, M.P., Martinez-Outschoorn, U.E., Sotgia, F., 2013. Oncogenes induce the cancer-associated fibroblast phenotype: metabolic symbiosis and "fibroblast addiction" are new therapeutic targets for drug discovery. Cell Cycle 12, 2723–2732. https://doi.org/10.4161/cc.25695.

Luchetti, A., Walsh, D., Rodger, F., Clark, G., Martin, T., Irving, R., Sanna, M., Yao, M., Robledo, M., Neumann, H.P., Woodward, E.R., Latif, F., Abbs, S., Martin, H., Maher, E.R., 2015. Profiling of somatic mutations in phaeochromocytoma and paraganglioma by targeted next generation sequencing analysis. Internet J. Endocrinol. 2015, 138573 https://doi.org/10.1155/2015/138573.

Martinez-Outschoorn, U.E., Lin, Z., Trimmer, C., Flomenberg, N., Wang, C., Pavlides, S., Pestell, R.G., Howell, A., Sotgia, F., Lisanti, M.P., 2011. Cancer cells metabolically

"fertilize" the tumor microenvironment with hydrogen peroxide, driving the Warburg effect: implications for PET imaging of human tumors. Cell Cycle 10, 2504–2520. https://doi.org/10.4161/cc.10.15.16585.

Martiniova, L., Lai, E.W., Elkahloun, A.G., Abu-Asab, M., Wickremasinghe, A., Solis, D.C., Perera, S.M., Huynh, T.T., Lubensky, I.A., Tischler, A.S., Kvetnansky, R., Alesci, S., Morris, J.C., Pacak, K., 2009. Characterization of an animal model of aggressive metastatic pheochromocytoma linked to a specific gene signature. Clin. Exp. Metastasis 26, 239–250. https://doi.org/10.1007/s10585-009-9236-0.

Matlac, D.M., Hadrava Vanova, K., Bechmann, N., Richter, S., Folberth, J., Ghayee, H.K., Ge, G.B., Abunimer, L., Wesley, R., Aherrahrou, R., Dona, M., Martínez-Montes, Á. M., Calsina, B., Merino, M.J., Schwaninger, M., Deen, P.M.T., Zhuang, Z., Neuzil, J., Pacak, K., Lehnert, H., Fliedner, S.M.J., 2021. Succinate mediates tumorigenic effects *via* succinate receptor 1: potential for new targeted treatment strategies in succinate dehydrogenase deficient paragangliomas. Front. Endocrinol. 12, 589451 https://doi.org/10.3389/fendo.2021.589451.

Moog, S., Lussey-Lepoutre, C., Favier, J., 2020. Epigenetic and metabolic reprogramming of SDH-deficient paragangliomas. Endocr. Relat. Cancer 27, R451–R463. https://doi.org/10.1530/ERC-20-0346.

Müller, U., Troidl, C., Niemann, S., 2005. SDHC mutations in hereditary paraganglioma/pheochromocytoma. Fam. Cancer 4, 9–12. https://doi.org/10.1007/s10689-004-0621-1.

Mulligan, L.M., Kwok, J.B., Healey, C.S., Elsdon, M.J., Eng, C., Gardner, E., Love, D.R., Mole, S.E., Moore, J.K., Papi, L., et al., 1993. Germ-line mutations of the RET proto-oncogene in multiple endocrine neoplasia type 2A. Nature 363, 458–460. https://doi.org/10.1038/363458a0.

Najafi, M., Mortezaee, K., Majidpoor, J., 2019. Stromal reprogramming: a target for tumor therapy. Life Sci. 239, 117049 https://doi.org/10.1016/j.lfs.2019.117049.

Olumi, A.F., Grossfeld, G.D., Hayward, S.W., Carroll, P.R., Tlsty, T.D., Cunha, G.R., 1999. Carcinoma-associated fibroblasts direct tumor progression of initiated human prostatic epithelium. Cancer Res. 59, 5002–5011. https://doi.org/10.1186/bcr138.

Qin, Y., Yao, L., King, E.E., Buddavarapu, K., Lenci, R.E., Chocron, E.S., Lechleiter, J.D., Sass, M., Aronin, N., Schiavi, F., 2010. Germline mutations in TMEM127 confer susceptibility to pheochromocytoma. Nat. Genet. 42, 229–233. https://doi.org/10.1038/ng.533.

Rapizzi, E., Ercolino, T., Canu, L., Giaché, V., Francalanci, M., Pratesi, C., Valeri, A., Mannelli, M., 2012. Mitochondrial function and content in pheochromocytoma/paraganglioma of succinate dehydrogenase mutation carriers. Endocr. Relat. Cancer 19, 261–269. https://doi.org/10.1530/ERC-11-0263.

Rapizzi, E., Ercolino, T., Fucci, R., Zampetti, B., Felici, R., Guasti, D., Morandi, A., Giannoni, E., Giaché, V., Bani, D., Chiarugi, A., Mannelli, M., 2014. Succinate dehydrogenase subunit B mutations modify human neuroblastoma cell metabolism and proliferation. Horm. Cancer 5, 174–184. https://doi.org/10.1007/s12672-014-0172-3.

Rapizzi, E., Fucci, R., Giannoni, E., Canu, L., Richter, S., Cirri, P., Mannelli, M., 2015. Role of microenvironment on neuroblastoma SK-N-AS SDHB-silenced cell metabolism and function. Endocr. Relat. Cancer 22, 409–417. https://doi.org/10.1530/ERC-14-0479.

Remacha, L., Currás-Freixes, M., Torres-Ruiz, R., Schiavi, F., Torres-Pérez, R., Calsina, B., Letón, R., Comino-Méndez, I., Roldán-Romero, J.M., Montero-Conde, C., 2018. Gain-offunction mutations in DNMT3A in patients with paraganglioma. Genet. Med. 20, 1644–1651. https://doi.org/10.1038/s41436-018-0003-y.

Remacha, L., Pirman, D., Mahoney, C.E., Coloma, J., Calsina, B., Currás-Freixes, M., Letón, R., Torres-Pérez, R., Richter, S., Pita, G., Herráez, B., Cianchetta, G., Honrado, E., Maestre, L., Urioste, M., Aller, J., García-Uriarte, Ó., Gálvez, M.Á., Luque, R.M., Lahera, M., Moreno-Rengel, C., Eisenhofer, G., Montero-Conde, C., Rodríguez-Antona, C., Llorca, Ó., Smolen, G.A., Robledo, M., Cascón, A., 2019. Recurrent germline DLST mutations in individuals with multiple pheochromocytomas and paragangliomas. Am. J. Hum. Genet. 104, 651–664. https://doi.org/10.1016/j.ajhg.2019.02.017.

Richter, S., Peitzsch, M., Rapizzi, E., Lenders, J.W., Qin, N., de Cubas, A.A., Schiavi, F., Rao, J.U., Beuschlein, F., Quinkler, M., Timmers, H.J., Opocher, G., Mannelli, M., Pacak, K., Robledo, M., Eisenhofer, G., 2014. Krebs cycle metabolite profiling for identification and stratification of pheochromocytomas/paragangliomas due to succinate dehydrogenase deficiency. J. Clin. Endocrinol. Metab. 99, 3903–3911. https://doi.org/10.1210/jc.2014-2151.

Richter, S., D'Antongiovanni, V., Martinelli, S., Bechmann, N., Riverso, M., Poitz, D.M., Pacak, K., Eisenhofer, G., Mannelli, M., Rapizzi, E., 2018. Primary fibroblast co-culture stimulates growth and metabolism in Sdhb-impaired mouse pheochromocytoma MTT cells. Cell Tissue Res. 374, 473–485. https://doi.org/10.1007/s00441-018-2907-x.

Schindelin, J., Arganda-Carreras, I., Frise, E., Kaynig, V., Longair, M., Pietzsch, T., Preibisch, S., Rueden, C., Saalfeld, S., Schmid, B., Tinevez, J.Y., White, D.J., Hartenstein, V., Eliceiri, K., Tomancak, P., Cardona, A., 2012. Fiji: an open-source platform for biological-image analysis. Nat. Methods 9, 676–682. https://doi.org/10.1038/nmeth.2019.

Selak, M.A., Armour, S.M., MacKenzie, E.D., Boulahbel, H., Watson, D.G., Mansfield, K. D., Pan, Y., Celeste Simon, M., Thompson, C.B., Gottlieb, E., 2005. Succinate links TCA cycle dysfunction to oncogenesis by inhibiting HIF-alpha prolyl hydroxylase. Cancer Cell 7, 77–85. https://doi.org/10.1016/j.ccr.2004.11.022.

Timmers, H.J., Kozupa, A., Eisenhofer, G., Raygada, M., Adams, K.T., Solis, D., Lenders, J.W., Pacak, K., 2007. Clinical presentations, biochemical phenotypes, and genotype-phenotype correlations in patients with succinate dehydrogenase subunit B-associated pheochromocytomas and paragangliomas. J. Clin. Endocrinol. Metab. 92, 779–786. https://doi.org/10.1210/jc.2006-2315.

Wallace, M.R., Marchuk, D.A., Andersen, L.B., Letcher, R., Odeh, H.M., Saulino, A.M., Fountain, J.W., Brereton, A., Nicholson, J., Mitchell, A.L., 1990. Type-1 neurofibromatosis gene: identification of a large transcript disrupted in three NF1 patients. Science 249, 181–186. https://doi.org/10.1126/science.2134734.

Warburg, O., Wind, F., Negelein, E., 1927. The metabolism of tumors in the body. J. Gen. Physiol. 8, 519–530. https://doi.org/10.1085/jgp.8.6.519.

Welander, J., Łysiak, M., Brauckhoff, M., Brunaud, L., Söderkvist, P., Gimm, O., 2018. Activating FGFR1 mutations in sporadic pheochromocytomas. World J. Surg. 42, 482–489. https://doi.org/10.1007/s00268-017-4320-0.

Wolf, K., Wu, Y.I., Liu, Y., Geiger, J., Tam, E., Overall, C., Stack, M.S., Friedl, P., 2007. Multi-step pericellular proteolysis controls the transition from individual to collective cancer cell invasion. Nat. Cell Biol. 9, 893–904. https://doi.org/10.1038/ncb1616.

Wu, T., Dai, Y., 2017. Tumor microenvironment and therapeutic response. Cancer Lett. 387, 61–68. https://doi.org/10.1016/j.canlet.2016.01.043.

Yang, Y., Zheng, H., Zhan, Y., Fan, S., 2019. An emerging tumor invasion mechanism about the collective cell migration. Am. J. Transl. Res 11, 5301–5312. www.ajtr.org/ISSN:1943-8141/AJTR0098753.

Zhang, J., Goliwas, K.F., Taufalele, P.V., Bordeleau, F., Reinhart-King, C.A., 2019. Energetic regulation of coordinated leader–follower dynamics during collective invasion of breast cancer cells. Proc. Natl. Acad. Sci. U.S.A. 16 (16), 7867–7872. https://doi.org/10.1073/pnas.1809964116, 116.

Zhu, J., Liang, L., Jiao, Y., Liu, L., 2015. Enhanced invasion of metastatic cancer cells via extracellular matrix interface. PLoS One 10, e0118058. https://doi.org/10.1371/journal.pone.0118058.

Zhuang, Z., Yang, C., Lorenzo, F., Merino, M., Fojo, T., Kebebew, E., Popovic, V., Stratakis, C.A., Prchal, J.T., Pacak, K., 2012. Somatic HIF2A gain-of-function mutations in paraganglioma with polycythemia. N. Engl. J. Med. 367, 922–930. https://doi.org/10.1056/NEJMoa1205119.